



OPEN ACCESS

EDITED BY

Liang Chen,
China University of Mining and
Technology, China

REVIEWED BY

Gang Lin,
École Normale Supérieure, France
Qihong Wu,
Chengdu University, China

*CORRESPONDENCE

An Chen,
✉ 20140025@kust.edu.cn
Kexin Yin,
✉ kexin.yin@nuaa.edu.cn

SPECIALTY SECTION

This article was submitted to
Environmental Informatics
and Remote Sensing,
a section of the journal
Frontiers in Earth Science

RECEIVED 20 November 2022

ACCEPTED 13 March 2023

PUBLISHED 23 March 2023

CITATION

Meng J, Chen A, Yin K and Zhou C (2023),
Study on the clogging mechanism of
upward inclined drainage holes in
cut slopes.
Front. Earth Sci. 11:1103323.
doi: 10.3389/feart.2023.1103323

COPYRIGHT

© 2023 Meng, Chen, Yin and Zhou. This is
an open-access article distributed under
the terms of the [Creative Commons
Attribution License \(CC BY\)](https://creativecommons.org/licenses/by/4.0/). The use,
distribution or reproduction in other
forums is permitted, provided the original
author(s) and the copyright owner(s) are
credited and that the original publication
in this journal is cited, in accordance with
accepted academic practice. No use,
distribution or reproduction is permitted
which does not comply with these terms.

Study on the clogging mechanism of upward inclined drainage holes in cut slopes

Jian Meng^{1,2}, An Chen^{2,3,4*}, Kexin Yin^{5*} and Caihui Zhou⁶

¹Kunming Prospecting Design Institute of China Nonferrous Metals Industry Co., Ltd., Kunming, China, ²Faculty of Land Resources Engineering, Kunming University of Science and Technology, Kunming, China, ³Yunnan Key Laboratory of Geohazard Forecast and Geocological Restoration in Plateau Mountainous Area, Kunming, China, ⁴Key Laboratory of Geohazard Forecast and Geocological Restoration in Plateau Mountainous Area, Ministry of Natural Resources of the People's Republic of China, Kunming, China, ⁵Department of Civil and Airport Engineering, Nanjing University of Aeronautics and Astronautics, Nanjing, China, ⁶Yunnan Geological Exploration and Development Corporation, Kunming, China

Since groundwater is one of the main factors that affect the stability of highway slopes in mountainous regions, a smooth drainage is of importance for the safety of cut slopes. After years of service, the cut slopes of highway are often characterized with drainage problems or even drainage failures that threaten the stability and safety. In this paper, the clogging mechanism of drainage holes in highway cut slopes is firstly clarified through on-site survey. The soil and blockage samples are collected from typical slopes for laboratory tests and analysis, and the results reveal that all the blockages are made of fine-grained particles from the slopes. Scanning electron microscope (SEM) images indicate that the blockages penetrate the drainage pipe wrappings to form the clogging. The combined effect of clayey soil, chemicals, and biological clogging exacerbate the clogging process around the drainage pipes. Laboratory tests are also performed to simulate the CaCO₃ crystal clogging around the drainage holes, and the microstructure of the clogged geotechnical screens and geotextiles is observed by scanning electron microscope as well. The results confirm that the amount of CaCO₃ crystal attached to the drainage pipe surface increases with the time. The single-layer structure of screens does not facilitate the three-dimensional clogging as in the case of geotextiles. After soaking in diluted hydrochloric acid at a pH of 5.0, there is no significant decrease of CaCO₃ crystals attached on the screens and geotextiles. However, the CaCO₃ decrease is apparent after soaking in the hydrochloric acid at a pH of 3.0. The clogging of drainage holes can be classified into two stages according to the laboratory tests and acid soaking, and the relationship and characteristics between the two stages are summarized.

KEYWORDS

highway cut slope, underground water, drainage hole, clogging mechanism, CaCO₃ crystal, microstructure

1 Introduction

The stability slope is a major issue for the highway engineering in mountainous area (Pantelidis, 2009; Subramanian et al., 2017; Latief and Zainal, 2019; Liu et al., 2021; Tsao et al., 2021). Since groundwater is one of the main factors that affect the deformation and stability of slopes, ensuring a smooth drainage is essential for the safety slopes (Castro et al., 2020; Nistor et al., 2020; Zhang et al., 2020; He et al., 2021). Water-rich slopes widely exist in highway engineering in South China. Due to the large annual precipitation, long rainy season, and high

groundwater level, the rock-soil body of the slope is often immersed below the groundwater level for a long period. The physical, chemical, and mechanical erosion induced by the groundwater have a coupled effect on the stability of rock-soil body in the slope (Jiao et al., 2005; Wu et al., 2008). Under the long-term action of groundwater, some components in the rock-soil materials may be washed away (Gu et al., 2015). As a result, the structural plane strength that determines the stability of the rock-soil body decreases, and the stability of the slope declines finally. The hydrodynamic pressure generated by the groundwater seepage increases the sliding force of the rock-soil mass within the slope. At the same time, the buoyancy effect of the high groundwater level decreases the slipping resistance of the rock-soil mass, which in turn leads to a decrease on the stability (Santoso et al., 2011; Zhang et al., 2011; Kaczmarek and Popielski, 2019).

In addition to the regular reinforcements, drainage devices on the surface or in the deep part of the cut slopes are often installed. For instance, the upward inclined drainage holes are the most widely used method (Cahyadi et al., 2018; Hongyue et al., 2019; Sun et al., 2021). Upward inclined drainage holes are usually installed by drilling holes with a small upward inclination from the slope surface into the deep part and inserting plastic drainage pipes into the holes for draining water (Guo et al., 2018). The plastic pipes could be unperforated to allow a water drainage from the end part inside the slope or collect drainage from the perforated section. Perforated drainage pipes are specially designed to prevent clogging or failure (Cao et al., 2021), for instance, to have a geotextile wrapped around (Mininger, 2010; Guo et al., 2018). After several years' running, cut slopes of early-built highways are often with problems of poor drainage or even drainage failures, resulting in unguaranteed stability and safety (Guo et al., 2018; Zhang et al., 2020). Therefore, studying the formation and development mechanism of the clogging in upward inclined drainage holes is of great significance for investigating new technologies to prevent or delay the clogging process, and to extend the effectiveness of drainage holes. It is also important for the stability of the cut slopes.

So far there is no literature to present detailed research on the clogging mechanism of the upward inclined drainage holes. In this paper, the slope drainage holes were investigated firstly by the on-site survey to locate the serious and typical drainage clogging sections for further study. The representative clogged drainage holes under different geological conditions were compared to determine the similarities and differences of the clogging mechanisms. The rock-soil mass, blockage soils, and water in the typical sections with clogged drainage holes were sampled and then analyzed in laboratory. Then, the chemical clogging tests were conducted with a consideration on the design and operation conditions of the upward inclined drainage holes, in order to reveal the chemical clogging mechanism and the development rules. The clogging of drainage holes can be classified into two stages according to the on-site survey, chemical clogging tests, and comprehensive analysis.

2 On-site survey and analysis

2.1 On-site survey

The highway section studied herein is on the Beijing-Hong Kong-Macau Expressway, starting from Xiaotang at the junction of

Hunan and Guangdong and ending at Gantang in the western suburbs of Shaoguan, with a total length of 109.9 km. The section was constructed from October 1998 to April 2003. An on-site survey of this studied area shows that the expressway is in a region with complicated geology conditions. The lithology conditions are highly heterogeneous, which is mainly consist of sandstone, siltstone, and argillaceous sandstone, with locally distributed shale, carbonaceous shale, and heavily weathered coal seam. The groundwater is mainly fissure water, and water seepage and mudflow widely exist on some parts of the slope. The middle section is karst-developed limestone with high liquid limit soils overlying. The studied section is rich in groundwater, and there is an outcrop of groundwater on many slopes along the expressway. In addition, karst caves and collapses can be found in the local region, and most of the groundwater is fissure water or karst water. The frequent landslides and other undesirable geological hazards are common to encounter such as debris flow or collapse in the research area, which pose high potential risks to the stability of the slopes and the serviceability of the highway.

The slopes studied in the paper are characterized with poor drainage or drainage failure, and the old drainage holes have worked more than 10 years (see Figure 1). Most of the clogged drainage holes are blocked with fine-grained soil, and chemical crystallization can be found in the blockages. Most of the drainage holes show traces of algae and other organisms on the surface. Preliminary analysis during the on-site survey shows that the main reasons for the clogging and drainage failure of the upward inclined holes are summarized as follows.

- 1) The composition of the rock-soil mass varies greatly, and the transfer of particles and chemical crystals within the slope can easily induce mechanical or chemical clogging in the drainage holes and on the geotextile.
- 2) There are obvious seasonal variations in the groundwater level of the slope. The upward inclined drainage holes work intermittently, i.e., only in rainy seasons or non-rainy seasons with sudden heavy rainfall. Thus, the geotextile is exposed to the atmosphere for a long period of time. Biological activities and variations in the redox environment can easily cause chemical and biological clogging on the geotextile. The mutual effect between physical, chemical, and biological clogging eventually accelerates the clogging process of the drainage holes.
- 3) Since the geotextile wrapped around the drainage pipes cannot be cleaned or replaced after the installation, the clogging continues until the drainage holes fail to work. In this way, the geotextile wrapped cannot prevent the clogging in the long time of running.

Most of the drainage holes in the research area are characterized by different degrees of clogging, and nine typical slope sections with serious drainage clogging were selected for further research. The drainage clogging in the selected slopes distributed in the three typical geological sections was statistically analyzed. As shown in Table 1, the slopes in all three sections show serious clogging problem. Cracks appear on the slopes, and groundwater seeps out through these cracks due to the failed drainage holes. The cracks and groundwater seepage decrease the stability of the slopes.

Based on the analysis on the long-time running drainage holes, most of the serious clogging occurred after about 3 years of working.

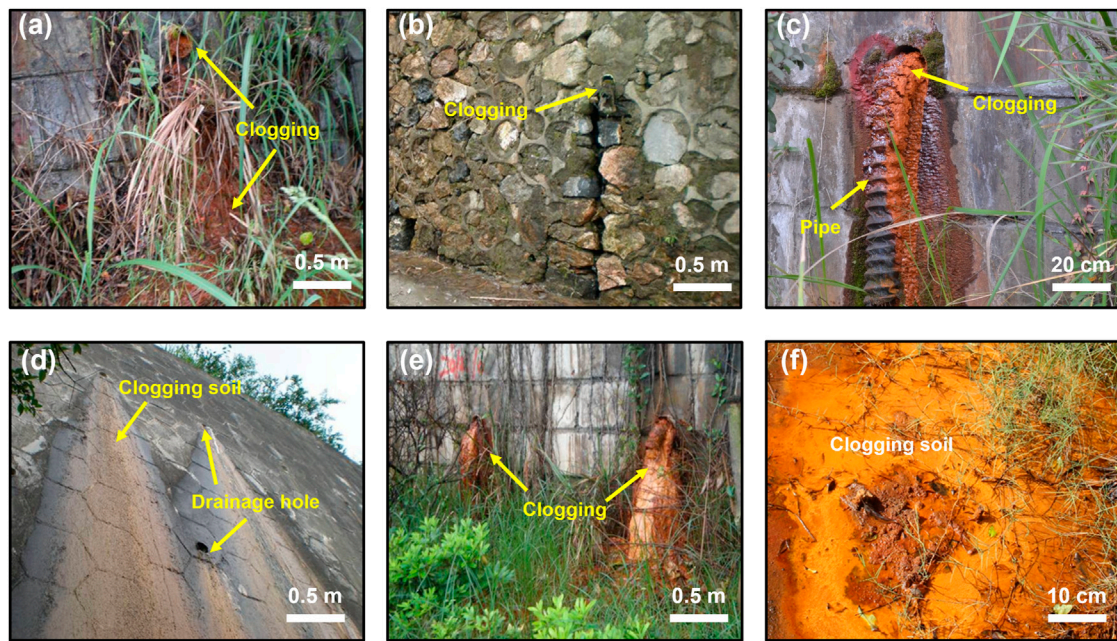


FIGURE 1
 Inclined drainage holes with poor drainage and clogging problem: **(A)** red clogging soil with plants; **(B)** brown clogging soil; **(C)** soft drainage pipe with red clogging soil; **(D)** clogging materials after rainfall; **(E)** totally clogging drainage holes; **(F)** red clogging soil near the drainage holes

TABLE 1 Cut slopes with clogged drainage.

No.	Marked work point number	Section with clogged drainage	Brief description of clogging
1	K1849+980~K1850+240 Right side slope	K1850+20~150 Primary slope	Water seepage and mudflow off the slope
2	K1858+930~K1859+260 Right side slope	K1858+950~K1859+000 Primary slope	Water seepage and mudflow off the slope
3	K1863+080~430 Left side slope	K1863+100~250 Primary slope	Water seepage and water flow from the retaining wall
		K1863+100~250 Secondary slope	Water seepage at the foot of the secondary slope
		K1863+100~250 Tertiary slope	Water seepage off the sidewall and anchor head of the slope
4	K1873+180~+350 Left side slope	K1873+270~310 Tertiary slope	Spalling of the mortared flagstone
5	K1876+280~670 Right side slope	K1876+430~+480 Primary slope	Local water seepage and mudflow, lush vegetation on the primary platform
		K1876+380~480 Secondary slope	Frequent water seepage and mudflow
6	K1881+160~300 Left side slope	K1881+200~240 Secondary slope	Water seepage in the middle and lower parts
		K1881+180~230 Foot of the slope	Water gushing at the roadbed side drainage ditch
7	K1918+225~385 Left side slope	K1918+225~385 Primary slope retaining wall	Perennial water flow at the lower and middle parts
8	K1925+550~875 Left side slope	K1925+550~875 Primary retaining wall	Multiple poor groundwater drainage
		K1925+550~875 Primary slope	Abundant water in the drainage ditch during the rainy season and water gushing off the masonry on both sides
9	K1941+000~440 Left side slope	K1941+000~440 Primary retaining wall	Severe water seepage

The average clogging time is 3.2 years according to a standard that the holes cannot drain water after a rainfall (see Table 2). New drainage holes are constructed on the clogging zone for later study and the stability of the slopes.

To analyze the typical clogging, three soil and three water samples were collected from each typical slope with clogged drainage holes for laboratory tests. The inner pipes were extracted from the representative clogged drainage holes, and the

TABLE 2 The information of the clogged drainage holes.

No.	Section with clogged drainage	The total number of drainage holes (–)	Average time to clogging (year)
1	K1850+20–150 Primary slope	86	2.81
2	K1858+950~K1859+000 Primary slope	34	3.01
3	K1863+100–250 Primary slope	98	2.51
	K1863+100–250 Secondary slope	98	2.88
	K1863+100–250 Tertiary slope	49	2.76
4	K1873+270–310 Tertiary slope	26	3.13
5	K1876+430~+480 Primary slope	30	2.93
	K1876+380–480 Secondary slope	60	3.21
6	K1881+200–240 Secondary slope	24	2.55
	K1881+180–230 Foot of the slope	16	2.01
7	K1918+225–385 Primary slope retaining wall	106	2.35
8	K1925+550–875 Primary retaining wall	160	3.35
	K1925+550–875 Primary slope	216	3.62
9	K1941+000–440 Primary retaining wall	220	4.11

blockage materials in the clogged drainage holes were also sampled for laboratory tests and analysis.

2.2 Analysis of drainage hole clogging mechanism

2.2.1 Analysis of blockage particles

Soil samples of the three typical slopes and their drainage hole blockages were collected for granulometric analysis. The particle size distribution curves were then obtained. Three slope soil samples and three drainage hole blockage samples were collected from each typical slope for testing, and the average values of every three samples were adopted for further analysis. The particle diameter of the slope soil varies greatly, while the blockages mostly consist of fine particles. Thus, both the sieving and densitometer methods were used to analyze the particle size distribution of the soil particles. As shown in Figure 2, the particle distribution curves from the average data of the three typical slope soil samples and the corresponding drainage hole blockages are compared: i.e., the right-side slope of K1858+930~K1859+260, the right-side slope of K1876+280–670, and the left-side slope of K1925+550–875 are presented here. The mark number K1858+930~K1859+260, K1876+280–670, and K1925+550–875 are renamed hereafter as K1858, K1876, and K1925, respectively.

According to the results from the above tests, the particle composition of the soil samples and drainage blockages of the three selected slopes is as follows.

- 1) The right-side slope of section K1858 is made of silty clay with grain size distribution shown in Figure 2A, in which the average soil content with a diameter below 0.075 mm is 66.0%. The drainage hole blockages are mainly clay, and

the content of soils with a diameter below 0.075 mm is 88.4% (Figure 2A).

- 2) The right-side slope of section K1876 is made of clay with grain size distribution shown in Figure 2B, in which the average content of particles below 0.075 mm is 69.5%. The drainage hole blockages are fine-grained soil (Figure 2B) with a diameter lower than 2 mm, of which the total content of particles below 0.075 mm is 83.2%.
- 3) The soil sample from the left slope of section K1925 is silt, mainly composed of sand and clay, and the content of soil particles below 0.075 mm is 39.8% (Figure 2C). The drainage hole blockages are mainly silt and clay, and the content of particles below 0.075 mm is 71.4% (Figure 2C).

Except for the left slope of the section K1925, the fine particle content in the soil of the other two slopes with clogged drainage holes is high, and the content of fine particles below 0.075 mm is above 65%. Although the fine particle content of the left slope of section K1925 is 26.2%–29.7% lower than the other two slopes (K1858 and K1876), the corresponding drainage hole blockages of all the three slopes are mainly fine-grained soil at high contents (71.4%–77.4%). The fine particle content in the drainage hole blockages is larger than that of the slope soil. Therefore, the drainage blockages are formed due to the fine particles from the side slope soil that are transported and accumulated by groundwater.

2.2.2 Chemical analysis of side slope soil and drainage blockage

Comparative compositional analysis of the slope soil and blockage samples was performed using X-ray fluorescence (XRF), which was simple to operate, non-destructive, fast, and accurate (Dos Anjos et al., 2000; Silva et al., 2019; Ravansari et al., 2020).

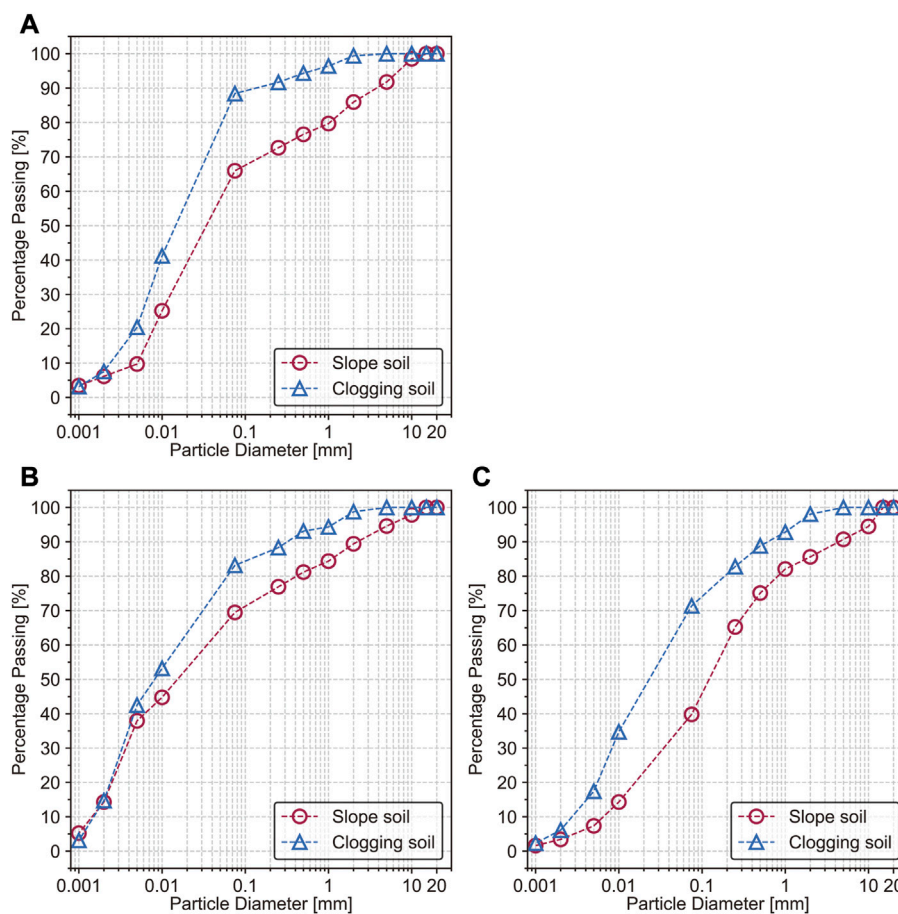


FIGURE 2 The particle size distribution of the three selected slope soil samples and their corresponding drainage hole blockages: (A) section K1858+930~K1859+260; (B) section K1876+280~670; (C) section K1925+550~875.

TABLE 3 Slope soil composition.

Sample	SiO ₂	Al ₂ O ₃	Na ₂ O	MgO	K ₂ O	CaO	MnO	Fe ₂ O ₃	TiO ₂	P ₂ O ₅	LOI
1858-S	57.2	21.9	0.09	1.87	2.66	0.04	0.02	5.65	0.66	0.05	9.3
1876-S	48.4	18.5	0.13	0.29	1.56	6.2	0.03	10.3	0.17	0.08	13.65
1925-S	50.81	18.4	0.08	1.08	1.24	1.57	0.44	8.51	0.32	0.15	16.42

TABLE 4 Blockage composition.

Sample	SiO ₂	Al ₂ O ₃	Na ₂ O	MgO	K ₂ O	CaO	MnO	Fe ₂ O ₃	TiO ₂	P ₂ O ₅	LOI
1858-B	19.40	5.50	0.14	0.06	0.24	0.22	0.109	58.71	0.03	0.20	15.41
1876-B	18.05	8.06	0.08	0.16	0.16	46.36	0.004	0.08	0.02	0.01	26.02
1925-B	20.81	7.69	0.20	0.08	0.33	2.25	0.464	49.38	0.14	0.09	18.56

Compositions of the three typical slope soil samples and drainage hole blockages are shown in Table 3 and Table 4, respectively.

According to the on-site survey, the drainage holes of section K1858 are located in a pelitic sandstone section, those of section

K1876 in the limestone section, and those of K1925 in the interbedded strata of shale, mudstone, and sandstone. A comparison of the compositions of soil samples from the three slopes and their drainage hole blockages indicates that.

TABLE 5 Water quality analysis.

No.	Ca ²⁺ (mg/L)	Mg ²⁺ (mg/L)	SO ₄ ²⁻ (mg/L)	PH
K1876-1	104.31	15.72	298.82	7.07
K1876-2	126.18	14.51	19.55	7.72
K1876-3	97.58	13.30	184.40	7.17

- 1) The composition of the drainage hole blockages in the three selected sections is the same as the slope soil, mainly silicon and aluminum oxides. Therefore, the clay content in the drainage hole blockages is high. Clay can promote mechanical clogging in the drainage hole. The fine-grained soil is the main material for mechanical clogging of drainage holes, which is also consistent with the results of particle distribution tests.
- 2) The calcium oxide content of the blockages in the limestone section K1876 is significantly higher than that in the corresponding slope soil, which may be attributed to the calcium precipitation around the drainage hole with intermittent groundwater outflow, i.e., the chemical clogging. At the same time, an analysis on the clogging materials in the newly running drainage holes finding that there is nearly no increase on the CaCO₃ crystals, indicating that the chemical clogging is developing in a low rate.
- 3) The iron oxide content of blockages in sections K1858 and K1925 is significantly higher than that in the slope. Therefore, Fourier Transform Infrared Spectroscopy (FTIR) analysis of the

samples is necessary to determine the iron composition (Hahn et al., 2018).

FTIR analysis on the blockage samples from sections K1858 and K1925 shows that the Fe in the blockage from section K1858 is possibly a mixture of Fe(OH)₃ and α-Fe₂O₃•H₂O. While the Fe in samples from K1925 is possibly Fe(OH)₃. On-site analysis of the water quality shows that the contents of free CO₂, erosive CO₂, and total dissolved solids are 50.18 mg/L, 34.17 mg/L, and 547.08 mg/L, respectively, making it moderately corrosive (pH = 4.5). The wire skeleton of flexible drainage pipes is generally corroded, and the same high Fe content is not detected in the blockages without flexible drainage pipes. Therefore, most of the Fe in the blockage comes from the wire skeleton of the flexible drainage pipes (Figure 1C), which is consistent with the conclusion that the ferrous blockage is mainly iron hydroxide and its transformations as indicated in the literature (Wu et al., 2007; Wu et al., 2008). Therefore, flexible drainage pipes have poor suitability for the research slope area.

A large number of calcium oxides is found in the blockages of the limestone section K1876. Water samples were collected from the slopes in this section for quality analysis to identify the chemical clogging mechanism of the drainage holes. The water quality analysis results of the slopes in the limestone section K1876 are shown in Table 5. The results show that all the groundwater within the slopes is SO₄²⁻-Ca²⁺-Mg²⁺ water, mostly neutral or alkaline water. However, the contents of SO₄²⁻, Ca²⁺, and Mg²⁺ vary significantly in the sampling places.

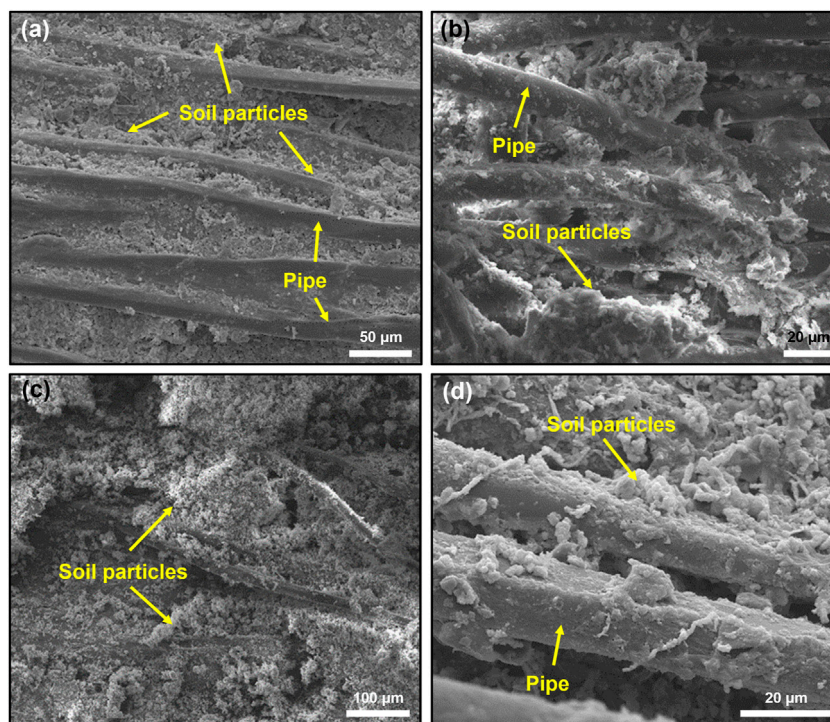


FIGURE 3 SEM images at the outer pipe end: (A), (B) inner surface; (C), (D) outer surface.

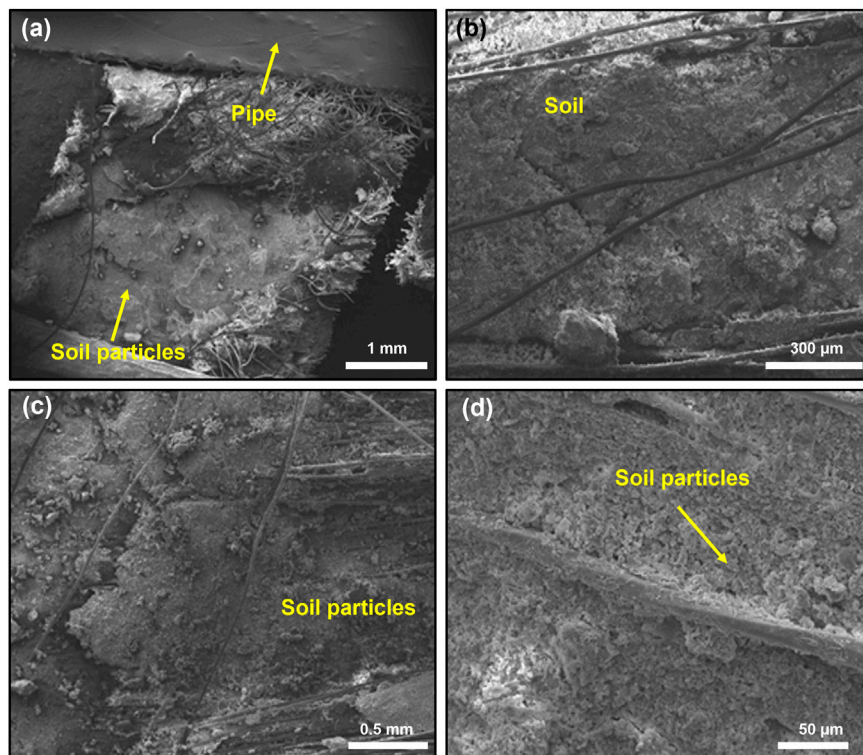


FIGURE 4
SEM images of the inner pipe end: (A), (B) inner surface; (C), (D) outer surface.

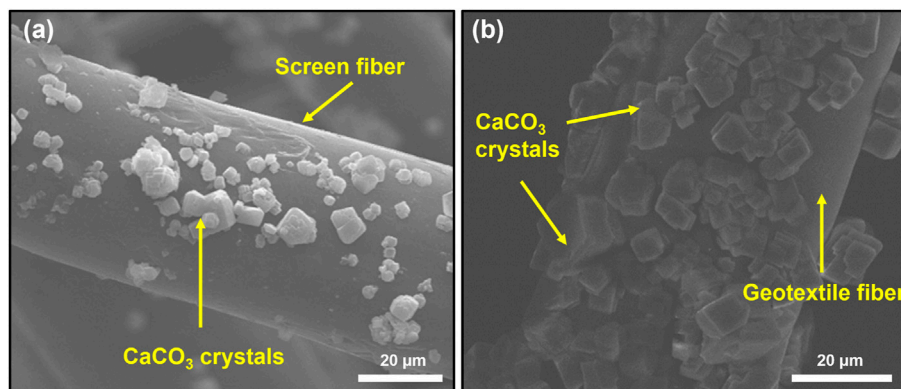


FIGURE 5
The attachment of CaCO_3 crystals on: (A) screen; (B) geotextile.

2.2.3 Scanning electron microscope test

Scanning electron microscope (SEM) is an effective method to investigate the microstructure of soils (Yin et al., 2019; Yin et al., 2021a; Yin et al., 2021b; Yin et al., 2021c; Yin, 2021). In order to further study the microstructure of the clogged drainage holes, SEM scans were performed on the inner and outer surfaces of the clogged drainage pipes at both ends (i.e., the outer and the inner pipe end). The images of the inner surface of the clogged

drainage pipes are shown in Figures 3A, B, and the outer surface images are presented in Figures 3C, D. The SEM results show significant differences between the blockages on the inside and outside surfaces of the outer section of the drainage pipes. The fiber on the inner surface is still clearly visible, while that on the outer surface is completely covered by the blockage. Therefore, the blockage materials gradually penetrate from the outer surface of the drainage pipes to the inner surface, and eventually reach

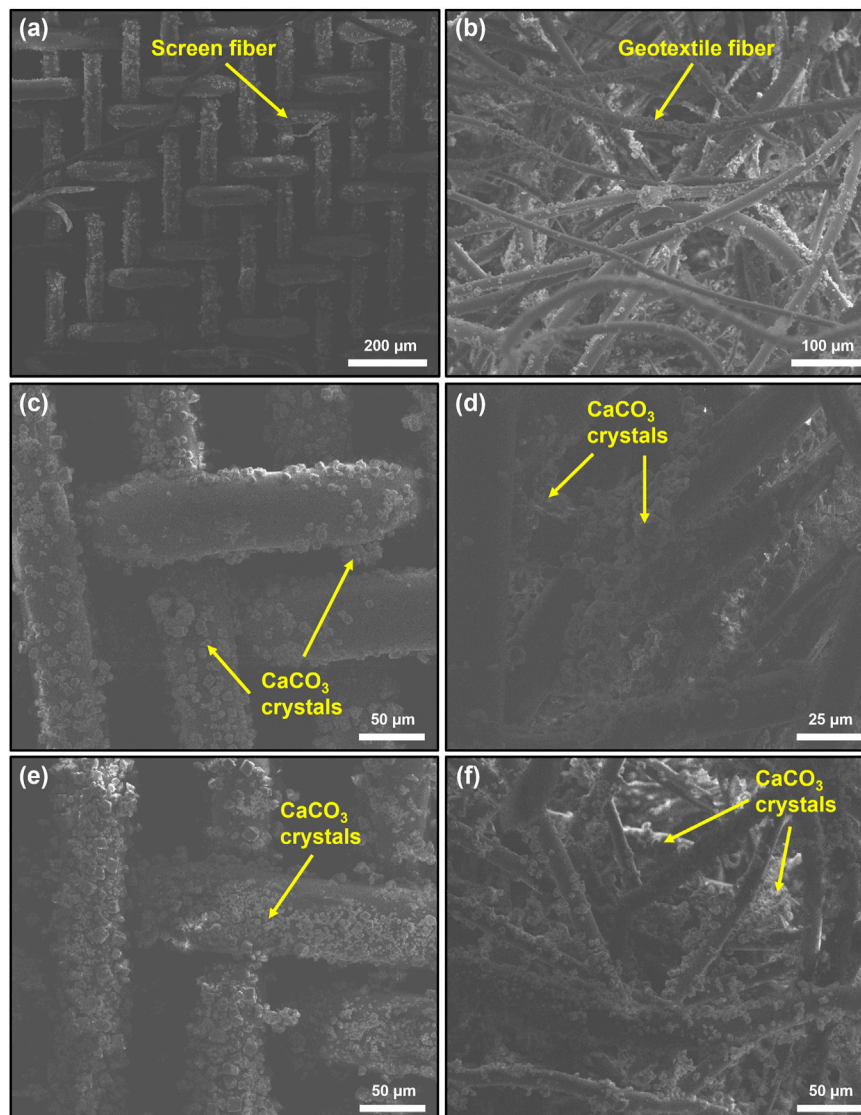


FIGURE 6

The screens and geotextiles under different titrations: (A), (B): 3 titrations; (C), (D): 6 titrations; (E), (F): 9 titrations.

saturation on the whole fiber. Thus, blockage materials are prevented from entering the interior and accumulating and just adhering to the outer surface of the drainage pipes.

Scanning images of the inner and outer surfaces of the inner pipe end are collected in Figure 4. Similar to the scans of the outer ends, at the inner end, fibers are visible on the inner surface but not on the outer surface. SEM images indicate more blockage at the inner end than the outer end of the drainage pipe (see Figure 3 and Figure 4). Therefore, the clogging of the drainage pipe at the inner pipe end is more severe than that at the outer end.

From the SEM images, we can see that the clogging develops from the materials wrapped (geotextile and screen). The fine particles transferred by the underground water accumulate on the wrapped geotextile and screen. More clogging is formed in the bottom of the drainage holes due to the transportation effect of the underground water.

3 Chemical clogging test

Since most of the drainage holes work for a short time throughout the year, chemical clogging is often neglected. Few studies focused on the chemical clogging in the side slopes, especially in limestone regions (Luquot et al., 2014). The above analysis on the clogging materials provide proofs for that chemical clogging in limestone regions is mainly in the form of CaCO_3 . Hence, it is necessary to perform model tests in the laboratory, to investigate the CaCO_3 chemical clogging mechanism as well as to know the distribution, arrangement and microstructure of the CaCO_3 crystal. Experiments of chemical clogging with different materials can offer useful information on drainage hole clogging improvements and delay or prevention of the chemical clogging.

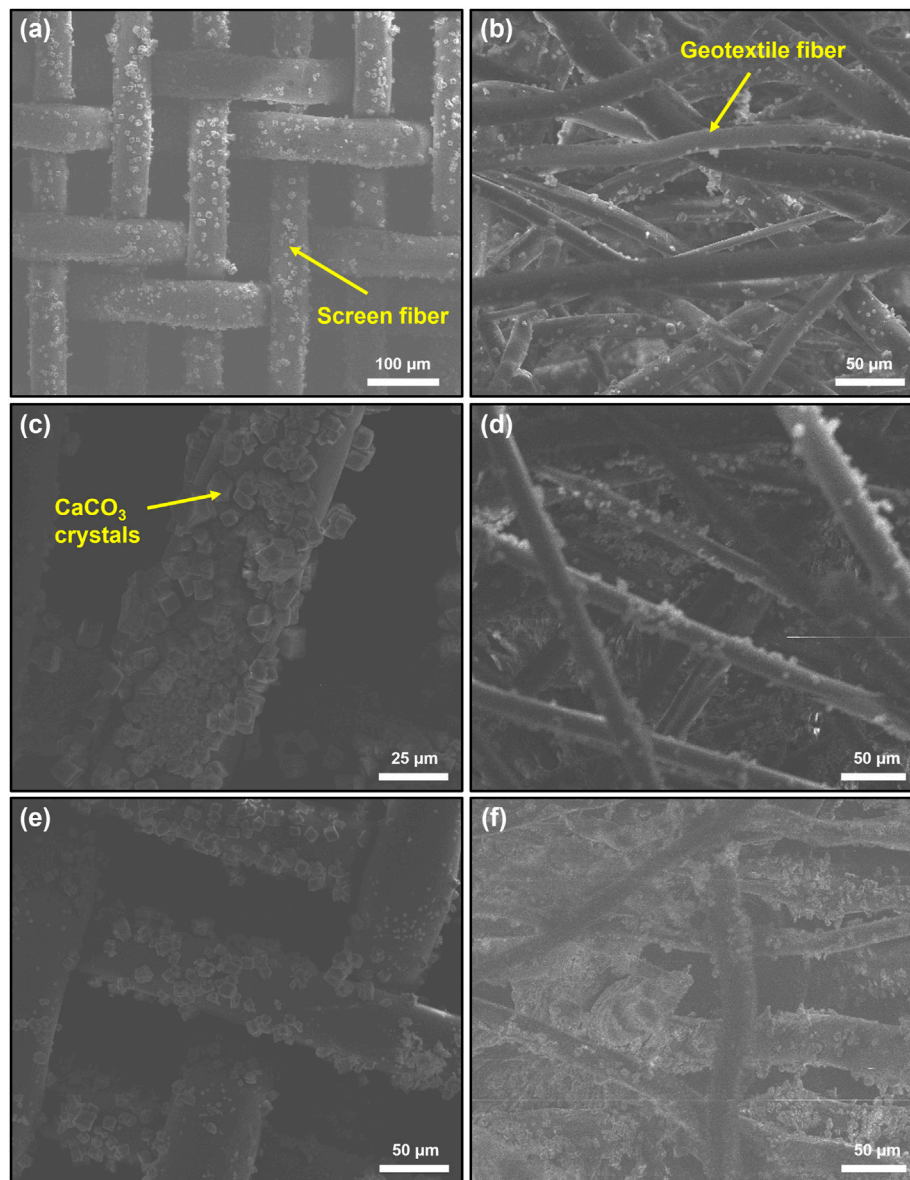
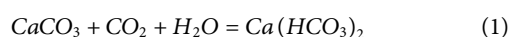


FIGURE 7
SEM images of the screens and geotextiles after: (A), (B): 3 titrations of acid washing; (C), (D): 6 titrations of acid washing; (E), (F): 9 titrations of acid washing.

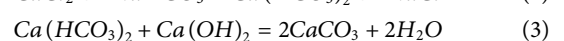
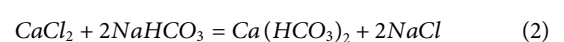
3.1 Experiment principle

Under the action of water and CO_2 , the abundant calcium ions in the groundwater undergo chemical dissolution, and the reaction equation is as follows:



$\text{Ca}(\text{HCO}_3)_2$ has a much higher solubility than CaCO_3 . With abundant groundwater and CO_2 , the water discharge from the side slope drainage holes generally contains more $\text{Ca}(\text{HCO}_3)_2$. However, the highly unstable $\text{Ca}(\text{HCO}_3)_2$ can be reduced to CaCO_3 precipitation under decreased pressure or increased temperature, which can easily block the drainage holes due to their mutual adhesion. In order to simulate the effects of calcium precipitates on the clogging process and

the clogging degree in the drainage holes (especially the outer wrapping of drainage pipes) of cut slopes, the highly soluble CaCl_2 solution was selected to provide Ca^{2+} , and NaHCO_3 solution was used to promote Ca^{2+} in generating $\text{Ca}(\text{HCO}_3)_2$ precipitation. Then, a certain amount of $\text{Ca}(\text{OH})_2$ was added to induce the conversion of $\text{Ca}(\text{HCO}_3)_2$ into the more stable CaCO_3 . The chemical formulas for the above reactions are as follows.



The above process was applied to the geotechnical screen and geotextile wrapped around the drainage pipes to simulate the calcareous blockage process. The geotechnical screen and geotextile were saved and sampled in steps, and SEM scanning

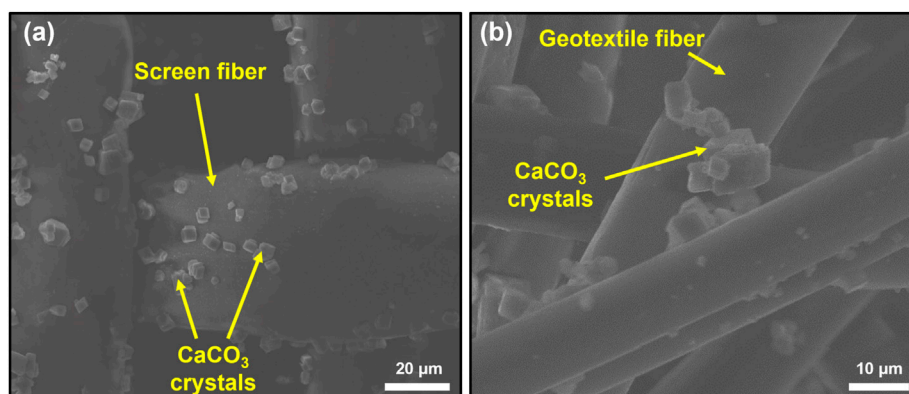


FIGURE 8
SEM images of the (A) screens and (B) geotextiles after 6 titrations of acid washing.

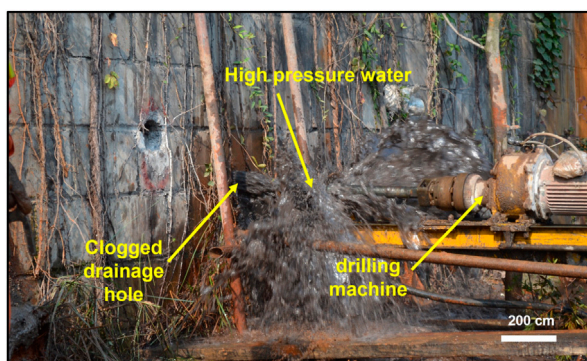
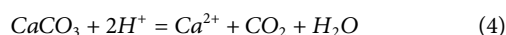


FIGURE 9
Drainage holes washing.

was performed to analyze the form and extent of clogging. Diluted acid was used to clean the screen and geotextile with chemical blockage, and the cleaning effect was observed as well. The reaction between the diluted acid and CaCO_3 is as follows:



3.2 Experimental setup

3.2.1 Equipment and chemicals

Several containers were needed to hold various chemical reagents for the experiment. Synthetic fiber screens (200 mesh) and geotextiles of different sizes were cut into $5.0 \text{ cm} \times 5.0 \text{ cm}$ for the experiment. The CaCO_3 crystallization adhered to the screens and geotextiles needed to be titrated with different acids and then compared. After the experiment, the screen and geotextile will be sampled for SEM scanning, which aims to reveal the internal microstructure and clarify the chemical clogging mechanism in the drainage holes and pipes. In addition, CaCl_2 , $\text{Ca}(\text{OH})_2$, $\text{Ca}(\text{HCO}_3)_2$, and HCl solutions of the required concentrations were prepared according to the experimental needs.

3.2.2 Experiment procedure

The detailed steps of the experiment are described as follows.

- 1) A 0.05 mol/L CaCl_2 solution, a 0.50 mol/L NaHCO_3 solution, a saturated $\text{Ca}(\text{OH})_2$ solution, and HCl solutions at pH of 3, 4, and five were prepared with distilled water.
- 2) The screen and geotextile were soaked in the 0.50 mol/L NaHCO_3 solution and then titrated with 0.05 mol/L CaCl_2 solution, followed by $\text{Ca}(\text{OH})_2$ solution. The screen and geotextile were dried after the reaction and then gently washed with distilled water to remove the soluble materials before being dried again. Two pieces of the screen and geotextile squares were sealed and stored: one for SEM scanning tests and the other for titration with a diluted acid. The rest of the screen and geotextile were used for subsequent experiments.
- 3) The dried screen and geotextile in Step 2 were titrated with the 0.50 mol/L NaHCO_3 solution until saturation and then titrated with the 0.05 mol/L CaCl_2 solution and $\text{Ca}(\text{OH})_2$ solution. The screen and geotextile were dried after the reaction and washed with distilled water to remove the soluble materials before being dried again. One of the screens and geotextiles was sealed and kept for SEM scanning, and the rest were used for subsequent experiments.
- 4) Step 3 was repeated until all screens and geotextiles were tested.
- 5) The screens and geotextiles in the above procedures saved for titration with diluted acid were subjected to diluted acid titration. Specifically, screens and geotextiles that underwent one precipitation test were titrated once, and those that underwent multiple precipitation tests were titrated an equal number of times to their number of precipitation. The phenomena that occurred during the test were observed, and the amount of diluted acid consumed was recorded. Then, the screens and geotextiles were dried and saved for SEM scanning.
- 6) Saturated CaCl_2 , NaHCO_3 , and $\text{Ca}(\text{OH})_2$ solutions were prepared at room temperature that is consistent with the *in situ* temperature, due to the changes of temperature will have impact on the chemical reactions (i.e., the higher temperature the faster reaction). Two screens and two geotextiles were soaked in NaHCO_3 solutions and then titrated with saturated CaCl_2 and

TABLE 6 Statistics of the drainage holes washing.

No.	Section with clogged drainage	Old failure holes (Recovered holes)	New holes (Recovered holes)
1	K1850+20–150 Primary slope	86 (12)	22 (9)
2	K1858+950~K1859+000 Primary slope	34 (9)	12 (5)
3	K1863+100–250 Primary slope	98 (6)	24 (11)
	K1863+100–250 Secondary slope	98 (22)	12 (7)
	K1863+100–250 Tertiary slope	49 (16)	12 (6)
4	K1873+270–310 Tertiary slope	26 (6)	9 (4)
5	K1876+430~+480 Primary slope	30 (16)	12 (7)
	K1876+380–480 Secondary slope	60 (22)	15 (8)
6	K1881+200–240 Secondary slope	24 (3)	6 (4)
	K1881+180–230 Foot of the slope	16 (2)	4 (4)
7	K1918+225–385 Primary slope retaining wall	106 (27)	20 (7)
8	K1925+550–875 Primary retaining wall	160 (25)	12 (10)
	K1925+550–875 Primary slope	216 (19)	30 (8)
9	K1941+000–440 Primary retaining wall	220 (42)	30 (14)
Success washing rate		18.6%	47.3%

Ca(OH)₂ solutions until the reaction was completed. The screens and geotextiles were dried and then washed with distilled water to remove the soluble materials before being dried again. One piece was saved for SEM scanning, and the other was titrated with diluted acid until the reaction was completed. The experimental phenomena were recorded.

- 7) All tested screens and geotextiles were subjected to the SEM scanning tests.

3.3 SEM results of chemical clogging

The screen and geotextile after the first two steps in Section 3 were scanned by SEM to observe the attachment of CaCO₃ crystals. Both the screen and the geotextile have CaCO₃ crystals attached to the fiber surface (see Figure 5). Under the *in situ* condition, as the working time of the drainage holes goes on, precipitated CaCO₃ crystals are accumulating on the screen and geotextile due to their high cohesiveness, thus exacerbating the clogging. From the distribution of the chemical clogging, it can be concluded that the wrapped materials with single-layer structure and larger pore size is more effective than these with multi-layer structure and smaller pore size to prevent the clogging.

The CaCO₃ crystal precipitation around the drainage holes with increasing *in situ* operation time was simulated by varying the number of CaCl₂ and Ca(OH)₂ titration. The images of the screens and geotextiles after titration are shown in Figure 6. A comparison of the microstructure of CaCO₃ precipitation indicates that the CaCO₃ crystals attached to the surface of the screen and the geotextile fibers increase with the increasing number of titrations. The CaCO₃ crystals continuously attach to and accumulate on the fibers, leading to blockage. With time going on, the crystal precipitation increases, and then chemical clogging intensifies.

The screens and geotextiles attached with CaCO₃ crystals were soaked in a diluted hydrochloric acid at a pH of 5.0 for 5 min, to observe the cleaning effect of acid washing on the chemical blockages. As presented in Figure 7, the decrease of CaCO₃ crystals attached to the screen and geotextile fibers was not significant after the acid washing with a pH = 5.0.

Since the decrease in the attached CaCO₃ crystals is not so significant after soaking in acid at the pH of 5.0, stronger hydrochloric acids are employed. SEM images of the screen and geotextile soaked with hydrochloric acid at a pH of 3.0 after 6 titrations are shown in Figure 8. The decrease in CaCO₃ crystals attached to the fibers is more significant after soaking in the stronger hydrochloric acid (pH = 3.0) for the same time (i.e., 5 min). Therefore, acid washing is effective for the Fe chemical blockage and Ca blockage.

4 Test of *in situ* drainage holes washing

The clogged drainage holes in the study area were washed from the outside to the inside with high-pressure water at a pressure of about 0.1 MPa (see Figure 9). After the washing, the cleaning effects on the old and new constructed drainage holes were counted and compared separately. The recovery of drainage after a rain is taken as the judging standard for the success of hole washing. The statistical success of hole washing is shown in Table 6. The data in brackets in the table is the number of drainage holes successfully washed. The operation time of the old drainage holes in this site is more than 10 years, and now it is in the late clogging stage, while the operation of the new drainage hole is working only for 2–3 years, i.e., the initial clogging stage. It can be seen from the statistical data that the drainage holes in the initial clogging stage are mainly physical blockage, and the success rate of washing reaches 47.3%. There

are blockage bonded together in the drainage holes located in the late clogging stage, due to the coupled effect of chemical and biological blockages. The Late clogging stage shows the characteristics of the three-dimensional comprehensive blockage. Therefore, the drainage effect of hole washing is not so effective, with a lower success rate of 18.6%.

5 Conclusion

In this paper, the degree and mechanism of drainage hole clogging in highway cut slopes were preliminarily clarified through an on-site survey. The soil and blockage samples from the selected slopes were collected for laboratory tests and analysis. The conclusions are summarized as follows.

- 1) All drainage holes in the research sections are characterized by different degrees of clogging. The blockages are correlated with the slope stratum lithology, the soil particle size, and the groundwater. All the blockages are made of fine-grained particles, and the clogging of slope drainage holes in slopes with clayey soil and other fine-grained soil is usually more severe. Slope drainage holes with flexible drainage pipes are also generally clogged with the hindered groundwater discharged, indicating its poor suitability for the slopes. The blockages contain abundant iron oxides, which are found to be related to the oxidation of the steel wire skeleton inside the flexible drainage pipes by FTIR analysis.
 - 2) SEM images show more blockages at the inner end of the drainage pipes than at the outer end and more blockages on the outside than on the inside of the drainage pipes, in agreement with the movement of underground water and the fine particles. The blockages penetrate deep inside the drainage pipe wrappings, and the combined effect of clayey soil, chemical clogging, and biological clogging exacerbate the clogging of drainage pipes with the increase in time.
 - 3) In addition to the same oxides as that in the side slopes, the blockages in the research area also have a high content of calcium oxides, indicating chemical clogging of calcium precipitates.
- The chemical clogging in the research area is mainly in the form of CaCO_3 crystals attached to the outer surface of the wrapping fibers, which exacerbates the clogging with its continuous accumulation. As a commonly used wrapping material for drainage pipes, the pore size of nylon screens is larger than that of geotextile. The single-layer structure of screens does not facilitate three-dimensional clogging without crystals attached to the interior. In contrast, geotextiles facilitate three-dimensional clogging with crystals attached to the different fibers. The three-dimensional clogging is difficult to clean through traditional washing methods. Therefore, under the same conditions, the chemical clogging of screens needs more time to form and is easier to clean than the chemical clogging of geotextiles.
- 4) Indoor tests were also conducted to simulate the CaCO_3 crystal precipitation clogging around the drainage holes in the research area, and the microstructure of the clogged screens and geotextiles was observed by using SEM. The main conclusions are in following: All chemical clogging on the screens and geotextiles is in the form of CaCO_3 crystal attachment and accumulation on

- the fiber surface, leading to severe clogging. The higher the number of titrations on the screens and geotextiles, the more CaCO_3 crystals is attached to the fiber surface. This study verifies that the amount of CaCO_3 crystals attached to the surface of the wrapping outside the drainage pipes increases with the operation time. Therefore, the effect of chemical clogging should be considered for the long-term operation of drainage holes. The decrease in CaCO_3 crystals attached to the screens and geotextiles is not significant after soaking in diluted hydrochloric acid at the pH of 5.0 but significant after soaking in hydrochloric acid at the pH of 3.0. Therefore, stronger acids perform better in removing part of the calcium clogging and delaying the chemical clogging. Considering the protection of environment, the acid washing method is not suggested to apply in the *in situ* engineering. The single-layer structure of screens does not facilitate three-dimensional clogging like in the geotextiles. In the meantime, the pore size of screens is larger than that of geotextiles. Therefore, chemical clogging on screens needs more time to form and is easier to clean than that in the geotextiles.
- 5) It can be seen from this study that drainage holes clogging can be divided into two typical stages: the initial stage and the late stage. The initial stage is dominated by physical blockage, which is manifested as fine grained soil that forming blockage around the drainage holes along with the groundwater migration. The physical blockage induced by fine grained soil is also a major component of the blockage. This stage is generally formed in an operation period of 2–3 years, and the drainage holes are often completely undrained. But there is usually a better hole washing effect on the drainage holes at this stage. With the increase of the operation time, the drainage holes are intermittently drained or even not drained, chemical and biological clogging become more obvious. The drainage holes located in the late stage make the blockage bond together to form a better whole because of chemical and biological blockage. Fine grained soil becomes difficult to destroy after bonding with chemicals, so the success rate of drainage hole washing at this stage is very low.
 - 6) The structure of the drainage hole makes the clogging inevitable, to make the permanent drainage effect better, it is necessary to invent a drainage hole that is less easily clogged or better washed. The existing drainage hole blockage is based on the drainage hole wrapping material, so improving the wrapping material or even cancelling the wrapping material will be an effective direction to reduce the drainage hole blockage or make the drainage hole easier to wash.

Data availability statement

The raw data supporting the conclusion of this article will be made available by the authors, without undue reservation.

Author contributions

JM, conceptualization, methodology, writing—original draft preparation, formal analysis; AC, conceptualization and methodology; KY, formal analysis, writing—original draft preparation, writing—review and editing; CZ, writing—review and editing. All authors have read and agreed to the published version of the manuscript.

Funding

This research is supported by the Talent Cultivation Project at Kunming University of Science and Technology (KKZ3201621012).

Conflict of interest

Author JM was employed by the Company Kunming Prospecting Design Institute of China Nonferrous Metals Industry Co., Ltd. Author CZ was employed by Yunnan Geological Exploration and Development Corporation.

References

- Cahyadi, T., Widodo, L., Fajar, R., and Baiquni, A. (2018). "Influence of drain hole inclination on drainage effectiveness of coal open pit mine slope," in *IOP conference series: Earth and environmental science* (IOP Publishing), 012060.
- Cao, Y., Xu, M., Ni, P., and Mei, G. (2021). Physical and numerical modelling of infiltration from drainage holes for perforated storm sewer. *Acta Geotech.* 17, 527–543. doi:10.1007/s11440-021-01247-0
- Castro, J., Asta, M. P., Galve, J. P., and Azañón, J. M. (2020). Formation of clay-rich layers at the slip surface of slope instabilities: The role of groundwater. *Water* 12 (9), 2639. doi:10.3390/w12092639
- Dos Anjos, M., Lopes, R., De Jesus, E., Assis, J., Cesareo, R., and Barradas, C. (2000). Quantitative analysis of metals in soil using X-ray fluorescence. *Spectrochim. Acta Part B At. Spectrosc.* 55 (7), 1189–1194. doi:10.1016/s0584-8547(00)00165-8
- Guo, Y., Leng, W., Nie, R., Zhao, C., and Zhang, X. (2018). Laboratory evaluation of a new device for water drainage in roadside slope along railway systems. *Geotext. Geomembranes* 46 (6), 897–903. doi:10.1016/j.geotextmem.2018.08.005
- Gu, T. F., Zhu, L. F., Hu, W., Wang, J. D., and Liu, Y. M. (2015). Effect on slope stability due to groundwater rising caused by irrigation: a case study of Heifang Platform in Gansu. *China. Geosci.* 29 (2), 408–413 (in Chinese).
- Hahn, A., Vogel, H., Andó, S., Garzanti, E., Kuhn, G., Lantzsich, H., et al. (2018). Using Fourier transform infrared spectroscopy to determine mineral phases in sediments. *Sediment. Geol.* 375, 27–35. doi:10.1016/j.sedgeo.2018.03.010
- He, Y., Sun, R., Xu, Z., and Tang, W. (2021). The dynamic change and effect of rainfall induced groundwater flow. *Water* 13 (19), 2625. doi:10.3390/w13192625
- Hongyue, S., Feixiang, S., Yuequan, S., Huan, X., and Dongfei, W. (2019). Study on negative pressure drainage method of down dip borehole in slope. *J. Eng. Geol.* 27 (3), 585–591.
- Jiao, J. J., Wang, X. S., and Nandy, S. (2005). Confined groundwater zone and slope instability in weathered igneous rocks in Hong Kong. *Eng. Geol.* 80 (1–2), 71–92. doi:10.1016/j.enggeo.2005.04.002
- Kaczmarek, Ł. D., and Popielski, P. (2019). Selected components of geological structures and numerical modelling of slope stability. *Open Geosci.* 11 (1), 208–218. doi:10.1515/geo-2019-0017
- Latief, R. H., and Zainal, A. K. E. (2019). Effects of water table level on slope stability and construction cost of highway embankment. *Eng. J.* 23 (5), 1–12. doi:10.4186/ej.2019.23.5.1
- Liu, Z., Liu, P., Zhou, C., and Zhang, L. (2021). A theoretical framework for optimization of three-dimensional slope stability monitoring. *Eng. Geol.* 295, 106436. doi:10.1016/j.enggeo.2021.106436
- Luquot, L., Roetting, T. S., and Carrera, J. (2014). Characterization of flow parameters and evidence of pore clogging during limestone dissolution experiments. *Water Resour. Res.* 50 (8), 6305–6321. doi:10.1002/2013wr015193
- Mininger, K. T. (2010). *Lifespan of horizontal wick drains used for landslide drainage*. Colorado School of Mines.
- Nistor, M. M., Rahardjo, H., Satyanaga, A., Hao, K. Z., Xiaosheng, Q., and Sham, A. W. L. (2020). Investigation of groundwater table distribution using borehole piezometer data interpolation: Case study of Singapore. *Eng. Geol.* 271, 105590. doi:10.1016/j.enggeo.2020.105590
- Pantelidis, L. (2009). Rock slope stability assessment through rock mass classification systems. *Int. J. Rock Mech. Min. Sci.* 46 (2), 315–325. doi:10.1016/j.ijrmmms.2008.06.003
- Ravansari, R., Wilson, S. C., and Tighe, M. (2020). Portable X-ray fluorescence for environmental assessment of soils: Not just a point and shoot method. *Environ. Int.* 134, 105250. doi:10.1016/j.envint.2019.105250
- Santoso, A. M., Phoon, K. K., and Quek, S. T. (2011). Effects of soil spatial variability on rainfall-induced landslides. *Comput. Struct.* 89 (11–12), 893–900. doi:10.1016/j.compstruc.2011.02.016
- Silva, E. A., Weindorf, D. C., Silva, S. H., Ribeiro, B. T., Poggere, G. C., Carvalho, T. S., et al. (2019). Advances in tropical soil characterization via portable X-ray fluorescence spectrometry. *Pedosphere* 29 (4), 468–482. doi:10.1016/s1002-0160(19)60815-5
- Subramanian, S. S., Ishikawa, T., and Tokoro, T. (2017). Stability assessment approach for soil slopes in seasonal cold regions. *Eng. Geol.* 221, 154–169. doi:10.1016/j.enggeo.2017.03.008
- Sun, H. Y., Ge, Q., Yu, Y., Shuai, F. X., and Lü, C. C. (2021). A new self-starting drainage method for slope stabilization and its application. *Bull. Eng. Geol. Environ.* 80 (1), 251–265. doi:10.1007/s10064-020-01918-4
- Tsao, M. C., Lo, W., Chen, W. L., and Wang, T. T. (2021). Landslide-related maintenance issues around mountain road in dasha river section of central cross island highway, taiwan. *Bull. Eng. Geol. Environ.* 80 (2), 813–834. doi:10.1007/s10064-020-01967-9
- Wu, J., Wu, Y., and Lu, J. (2008). Laboratory study of the clogging process and factors affecting clogging in a tailings dam. *Environ. Geol.* 54 (5), 1067–1074. doi:10.1007/s00254-007-0873-9
- Wu, J., Wu, Y., Lu, J., and Lee, L. (2007). Field investigations and laboratory simulation of clogging in Lixi tailings dam of Jinduicheng, China. *Environ. Geol.* 53 (2), 387–397. doi:10.1007/s00254-007-0654-5
- Yin, K., Fauchille, A. L., Di Filippo, E., Kotronis, P., and Sciarra, G. (2021a). A review of sand-clay mixture and soil-structure interface direct shear test. *Geotechnics* 1 (2), 260–306. doi:10.3390/geotechnics1020014
- Yin, K., Fauchille, A. L., Di Filippo, E., Othmani, K., Branchu, S., Sciarra, G., et al. (2021b). The influence of mixing orders on the microstructure of artificially prepared sand-clay mixtures. *Adv. Mater. Sci. Eng.* 2021, 1–15. doi:10.1155/2021/8552224
- Yin, K., Fauchille, A. L., Othmani, K., Sciarra, G., Kotronis, P., Benoit, Y., et al. (2019). "Influence of sample preparation on the multi scale structure of sand-clay mixtures," in *E3S Web of conferences* (EDP Sciences), 01007.
- Yin, K. (2021). Influence of clay fraction on the mechanical behavior of a soil-concrete interface. Nantes, France: Thesis. École centrale de Nantes.
- Yin, K., Liu, J., Lin, J., Vasilescu, A. R., Othmani, K., and Di Filippo, E. (2021c). Interface direct shear tests on JEZ-1 mars regolith simulant. *Appl. Sci.* 11 (15), 7052. doi:10.3390/app11157052
- Zhang, L., Zhang, J., Zhang, L., and Tang, W. H. (2011). Stability analysis of rainfall-induced slope failure: A review. *Proc. Institution Civ. Engineers-Geotechnical Eng.* 164 (5), 299–316. doi:10.1680/geng.2011.164.5.299
- Zhang, S., Xu, Q., Peng, D., Zhu, Z., Li, W., Wong, H., et al. (2020). Stability analysis of rock wedge slide subjected to groundwater dynamic evolution. *Eng. Geol.* 270, 105528. doi:10.1016/j.enggeo.2020.105528